A Model for Protein Translation: Polysome Self-Organization Leads to Maximum Protein Synthesis Rates

Hermioni Zouridis* and Vassily Hatzimanikatis†
*Department of Chemical and Biological Engineering, McCormick School of Engineering and Applied Sciences, Northwestern University, Evanston, Illinois; and †Laboratory of Computational Systems Biotechnology, Ecole Polytechnique Fédérale de Lausanne, Lausanne, Switzerland

ABSTRACT The genetic information in DNA is transcribed to mRNA and then translated to proteins, which form the building blocks of life. Translation, or protein synthesis, is hence a central cellular process. We have developed a gene-sequence-specific mechanistic model for the translation machinery, which accounts for all the elementary steps of the translation mechanism. We performed a sensitivity analysis to determine the effects of kinetic parameters and concentrations of the translational components on protein synthesis rate. Utilizing our mathematical framework and sensitivity analysis, we investigated the translational kinetic properties of a single mRNA species in *Escherichia coli*. We propose that translation rate at a given polysome size depends on the complex interplay between ribosomal occupancy of elongation phase intermediate states and ribosome distributions with respect to codon position along the length of the mRNA, and this interplay leads to polysome self-organization that drives translation rate to maximum levels.

INTRODUCTION

Translation, or protein synthesis, is a process that is central to cellular function and well conserved among all living organisms. It is one of processes in the ''central dogma'' of molecular biology and the last step in information transfer from DNA to protein. Decades of experimentation have elucidated a vast wealth of molecular information about discrete translation steps, but the sheer complexity of the translation mechanism necessitates that these results be integrated in a systematic framework for us to better understand the system properties of translation and make quantitative predictions.

Translation is essentially a template polymerization process (1) consisting of initiation, elongation, and termination phases. Messenger RNA (mRNA), composed of a sequence of codons coding for amino acids, carries genetic information. Initiation occurs with binding of the ribosome to the ribosomal binding site. During elongation the ribosome facilitates assembly of the polypeptide chain with one amino acid (aa) added per elongation step. Termination involves release of the completed peptide from the ribosome. Multiple proteins can be synthesized simultaneously on a single mRNA molecule, forming a structure called the polysome (or polyribosome) consisting of several ribosomes simultaneously translating the same mRNA. Polysome size is the number of ribosomes bound to a single mRNA molecule. Hence, the higher the polysome size, the greater the coverage of the mRNA due to ribosomes translating it. Polysomes have been observed experimentally (2), and modern techniques have allowed the quantification of polysome size for almost every mRNA in yeast cells (3).

Several studies have been conducted involving investigating the kinetics of protein synthesis that take into account the ribosome movement on mRNAs. Using a lattice model, MacDonald and others (4) and MacDonald and Gibbs (5) are among the first to model protein synthesis at the ribosome movement level. They consider multiple mRNAs of the same species to be one-dimensional lattices on which simultaneous peptide-chain elongation occurs. This work is extended by Heinrich and Rapoport (6) and accurately describes the phenomenon of ribosome crowding on an mRNA template. In recent work, Mehra and Hatzimanikatis (7,8) study properties of genome scale translation networks by using both simplified models (7) and the Heinrich and Rapoport (6) modeling framework (8). In these studies, the effects of competition for ribosomes between mRNAs on cell-wide mapping between mRNA and protein levels are investigated, and the correlation between mRNA and protein levels is determined to be a function of both kinetic parameters and ribosome concentration.

Previous mechanistic frameworks predict translation kinetics by capturing the interplay between initiation, elongation, and termination. An assumption in these studies is that the elongation kinetics at each codon depends on a single rate constant that is the same for all codon species at all positions along the length of the mRNA. In reality, codons have varying elongation kinetics due to different tRNA availabilities (9) and codon-anticodon compatibilities (10, 11), and the multiple elementary steps and translational components involved in the elongation cycle at every codon. Therefore, a better understanding of the properties of translation requires the consideration of the translation elongation phase, accounting for all elongation cycle intermediate steps.

In this work, we have developed a deterministic, sequence-specific kinetic model of the translational machinery

Submitted June 28, 2006, and accepted for publication August 29, 2006.

Address reprint requests to V. Hatzimanikatis, Tel.: 41-0-21-693-98-70; E-mail: vassily.hatzimanikatis@epfl.ch or vassily@northwestern.edu.

0006-3495/07/02/717/14 $2.00

doi: 10.1529/biophysj.106.087825

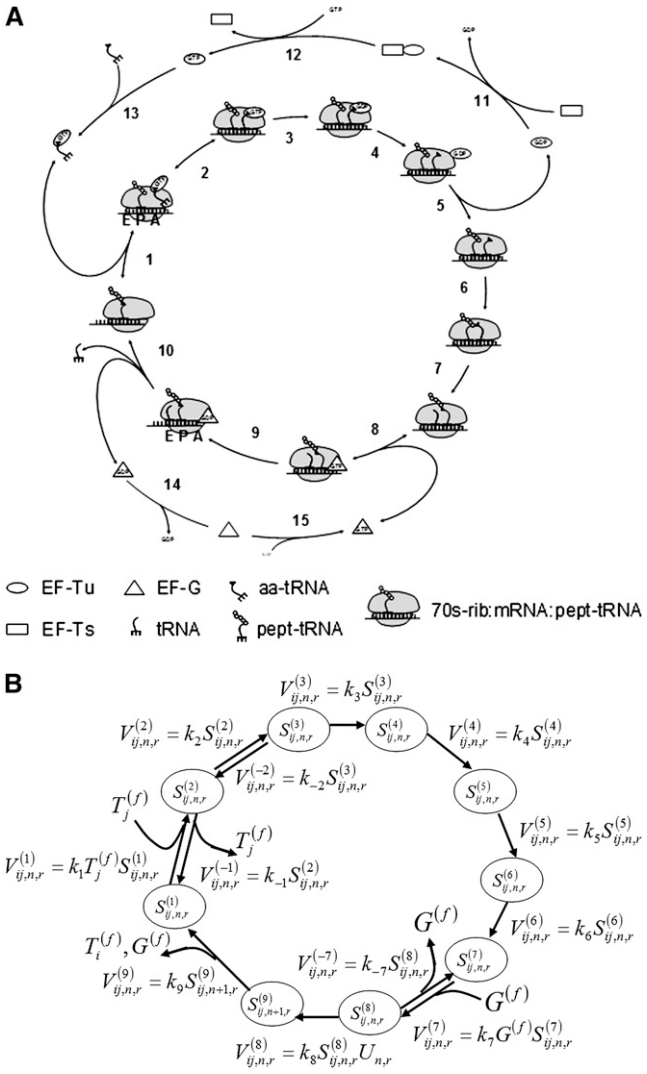

FIGURE 1 (*A*) The elementary mechanistic steps of the translation elongation process. Ribosomal A, P, and E sites indicated on the intermediates between Steps 1 and 2 and Steps 9 and 10. Step 1, Reversible, codon-independent binding of the ternary complex to the ribosomal A site. Step 2, Reversible, codon-dependent binding of the ternary complex to the ribosomal A site. Step 3, GTP hydrolysis. Step 4, Ef-Tu:GDP position change on the ribosome. Step 5, Ef-Tu:GDP release. Step 6, aa-tRNA accommodation. Step 7, Transpeptidation. Step 8, Reversible binding of Ef-G:GTP. Step 9, Translocation. Step 10, E site tRNA release. Steps 11 and 12, Ef-Ts catalyzed regeneration of Ef-Tu:GTP. Step 13, Ef-Tu:GTP binding to the aa-tRNA. Steps 14 and 15, Regeneration of Ef-G:GTP. (*B*) A graphical representation of the elementary elongation steps of the translation elongation process with nomenclature from the model formulation as explained in the text. Fluxes $V^{(1)}_{\mathrm{ij,n,r}}$ and $V^{(-1)}_{\mathrm{ij,n,r}}$ represent reversible, codon-independent binding of the ternary complex to the ribosomal A site. Fluxes $V^{(2)}_{\mathrm{ij,n,r}}$ and $V^{(-2)}_{\mathrm{ij,n,r}}$ represent reversible, codon-dependent binding of the ternary complex to the ribosomal A site. Flux $V^{(3)}_{\mathrm{ij,n,r}}$ represents GTP hydrolysis. Fluxes $V^{(4)}_{\mathrm{ij,n,r}}$ and $V^{(5)}_{\mathrm{ij,n,r}}$ represent Ef-Tu:GDP position change on the ribosome and Ef-Tu:GDP release, respectively. Flux $V^{(6)}_{\mathrm{ij,n,r}}$ represents aa-tRNA accommodation. Fluxes $V^{(7)}_{\mathrm{ij,n,r}}$ and $V^{(-7)}_{\mathrm{ij,n,r}}$ represent reversible binding of Ef-G:GTP. Flux $V^{(8)}_{\mathrm{ij,n,r}}$ represents ribosomal translocation. Flux $(V^{(9)}_{\mathrm{ij,n,r}})$ represents E site tRNA release. The intermediate elongation cycle states that occur before and after transpeptidation (Step 7, panel *A*) are considered to be one state in our model $(S^{(7)}_{\mathrm{ij,n,r}})$. After release of the tRNA in the ribosomal E site $(V^{(9)}_{\mathrm{ij,n,r}})$, the subsequent elongation cycle is ready to begin with the ribosomal P site positioned at codon $n+1$.

that accounts for all the elementary steps of the translation mechanism. Specifically, our model includes all the elementary steps involved in the elongation cycle at every codon along the length of the mRNA. We performed a sensitivity analysis to determine the effects of the kinetic parameters and concentrations of the translational components on the protein synthesis rate. Utilizing our mechanistic framework and sensitivity analysis, we investigate the steady-state protein synthesis properties of a single mRNA species. We determine the protein synthesis rate as a function of polysome size and then identify ranges of polysome sizes in which the translation kinetics are initiation-, elongation-, and termination-limited. Additionally, we investigate how ribosomes are distributed with respect to elongation cycle intermediate state and sequence position under initiation-, elongation-, and termination-limited regimes. To understand how each elongation cycle elementary step contributes to the kinetics of a given elongation cycle, we introduce a reduced version of our model. We propose that translation rate at a given polysome size depends on the complex interplay between ribosomal occupancy of elongation cycle intermediate states and ribosome distributions with respect to codon position along the length of the mRNA, and this interplay leads to polysome self-organization that drives translation rate to maximum levels.

METHODS

Elementary steps of the elongation cycle

The translation elongation phase is a cyclic process that involves codons, ribosomes, amino acids, tRNAs, elongation factors Tu, Ts, and G, and leads to the assembly of polypeptide chains (Fig. 1 *A*). Each aminoacyl-tRNA (aa-tRNA) binds to Ef-Tu:GTP, forming a ternary complex (Step 13). The ternary complex then binds reversibly to the ribosomal A site in a codon-independent manner (Step 1). After finding the correct codon match and reversible codon-dependent binding (Step 2), GTP is hydrolyzed (Step 3), Ef-Tu:GDP changes position on the ribosome (Step 4), and is released (Step 5). In a two-step process, Ef-Ts catalyze regeneration of Ef-Tu:GTP (Steps 11 and 12). During accommodation, the aa-tRNA undergoes a conformation change and enters the A site (Step 6). Transpeptidation then occurs (Step 7), where the peptide chain is transferred from the peptidyl-tRNA to the aa-tRNA, resulting in the elongation of the polypeptide chain by one amino acid. Reversible binding of Ef-G:GTP (Step 8) facilitates translocation (Step 9). During translocation the P site tRNA and codon move to the E site of the ribosome and the A site tRNA and codon move to the P site, resulting in the complex moving toward the 3′ end of the mRNA by one codon. The tRNA in the E site is released along with Ef-G:GDP (Step 10), and Ef-G:GTP is recycled in a two-step process (Steps 14 and 15).

Model formulation

We have employed the following assumptions in the formulation of the mathematical model for the elongation cycle. A graphical representation of the elementary steps of the elongation cycle with nomenclature from the model formulation is included in Fig. 1 *B*.

Assumption 1: The elongation cycle is modeled in terms of the states of the ribosome

Ribosomes at different stages of the elongation cycle are considered to be separate states, $S^{(\sigma)}_{ij,n,r}$. Each state σ is of type ij, where i is the codon species occupying the P site and j is the codon species occupying the A site, and n denotes the position of the ribosomal P site codon. Ribosomes are bound to mRNA species r, with $r \in M$, and M is the set of mRNA species. Codon positions along mRNA sequences are numbered from 1 to N_r starting at the 5′ end of the protein-coding region; N_r denotes the number of codons (length) of mRNA species r.

Assumption 2: Ribosomes cover 12 codons on the mRNA

We assume that a ribosome covers $L = 12$ codons on an mRNA (12–14), where L is the length of the ribosome. The front and back of the ribosome are defined to be on the sides closest to the 3′ and 5′ ends of the mRNA, respectively, with the A and P sites covering the sixth and seventh codons relative to the front of the ribosome. Hence, in addition to the codons occupying the ribosomal A and P sites in an elongation cycle state, the five codons preceding and following the A and P site codons are also covered by the ribosome.

Assumption 3: All free tRNAs are in the form of ternary complexes

Because most tRNAs are charged (15), Ef-Tu is present in a one-to-one ratio with tRNA (1), and the association rate constant of Ef-Tu:GTP to charged tRNAs is very high (16), we consider all free tRNAs to be in the form of ternary complexes. Free ternary complex concentrations ($T^{(f)}_k$) are of species k, with $k \in K$, where K is the set of ternary complex species. This assumption can be relaxed by including flux expressions corresponding to ternary complex formation.

Assumption 4: The set of reaction rate constants governing the kinetics of the intermediate elongation cycle steps are the same for all codons

We assume that every elongation cycle, regardless of the ternary complex species that binds to the ribosomal A site, the tRNA occupying the ribosomal P site, and the codon species occupying the A and P sites, have the same elementary steps and the same rate constants for each elementary step. Although experimental evidence suggests synonymous codons translated by the same tRNA are not necessarily translated at the same rate (10,11), rate constants specific to each codon species have yet to be determined. Hence, in the absence of this information, the same set of reaction rate constants (Table 1) adapted from the literature (17–20) were applied to the flux expressions (Table 2) of the intermediate steps of all elongation cycles. We assume the temperature and Mg concentration to be 37°C and 7 mM, respectively, so the reaction rate constants not determined experimentally at these conditions were adjusted accordingly.

Assumption 5: Ternary complex binding kinetics is first-order with respect to free ternary complex concentrations and the ribosomal state having the A site empty

The elongation cycle begins with binding of the ternary complex ($T^{(f)}_k$) to state 1, which is the ribosomal state having the A site empty ($S^{(1)}_{ij,n,r}$), to form state 2 ($S^{(2)}_{ij,n,r}$). This step corresponds to flux $V^{(1)}_{ij,n,r}$. State 2 represents nonspecific binding of ternary complexes to the A site.

Assumption 6: Only ternary complexes cognate to the A-site codon bind to the ribosome during nonspecific binding

Although ternary complexes can be incorrectly bound to noncognate codons at this point in the elongation cycle, for simplicity we assume that the concentration of incorrectly bound ternary complexes to the A site is comparatively small and consider state 2 to consist only of correctly bound ternary complexes to the A site. However, this assumption can be relaxed by adding additional states to the model.

TABLE 1 Kinetic parameters

Parameter	Definition	Characteristic value
k_1	Rate constant of ternary complex codon-independent binding*†	100 μM^{-1} s^{-1}
k_{-1}	Rate constant of ternary complex codon-independent binding reverse reaction*†	79 s^{-1}
k_2	Rate constant of ternary complex codon-dependent binding*†	207 s^{-1}
k_{-2}	Rate constant of ternary complex codon-dependent binding reverse reaction*†	3.45 s^{-1}
k_3	Rate constant of GTP hydrolysis‡	100 s^{-1}
k_4	Rate constant of Ef-Tu:GDP position change on the ribosome*	638 s^{-1}
k_5	Rate constant of Ef-Tu:GDP release*	15 s^{-1}
k_6	Rate constant of A site tRNA accommodation‡	20 s^{-1}
k_7	Rate constant of Ef-G:GTP binding¶	150 μM^{-1} s^{-1}
k_{-7}	Rate constant of Ef-G:GTP binding reverse reaction¶	140 s^{-1}
k_8	Rate constant of ribosome translocation¶	250 s^{-1}
k_9	Rate constant of E site tRNA release¶	20 s^{-1}
$k_{I,r}$	Translation initiation rate constant	Allowed to vary
$k_{T,r}$	Translation termination rate constant	Allowed to vary

*From Pape et al. (19).
†From Rodnina et al. (18) (activation energies were used to adjust rate constants for temperature).
‡From Bilgin et al. (17).
¶From Savelsburgh et al. (20).

TABLE 2 Flux expressions

Flux	Expression	Description
$V^{(1)}_{ij,n,r}$	$k_1 T^{(f)}_j S^{(1)}_{ij,n,r}$	Ternary complex codon-independent binding
$V^{(-1)}_{ij,n,r}$	$k_{-1} S^{(2)}_{ij,n,r}$	Ternary complex codon-independent binding reverse reaction
$V^{(2)}_{ij,n,r}$	$k_2 S^{(2)}_{ij,n,r}$	Ternary complex codon-dependent binding
$V^{(-2)}_{ij,n,r}$	$k_{-2} S^{(3)}_{ij,n,r}$	Ternary complex codon-dependent binding reverse reaction
$V^{(3)}_{ij,n,r}$	$k_3 S^{(3)}_{ij,n,r}$	GTP hydrolysis
$V^{(4)}_{ij,n,r}$	$k_4 S^{(4)}_{ij,n,r}$	Ef-Tu:GDP position change on the ribosome
$V^{(5)}_{ij,n,r}$	$k_5 S^{(5)}_{ij,n,r}$	Ef-Tu:GDP release
$V^{(6)}_{ij,n,r}$	$k_6 S^{(6)}_{ij,n,r}$	A site tRNA accommodation
$V^{(7)}_{ij,n,r}$	$k_7 G^{(f)} S^{(7)}_{ij,n,r}$	Ef-G:GTP binding
$V^{(-7)}_{ij,n,r}$	$k_{-7} S^{(8)}_{ij,n,r}$	Ef-G:GTP binding reverse reaction
$V^{(8)}_{ij,n,r}$	$k_8 S^{(8)}_{ij,n,r} U_{n,r}$	Ribosome translocation
$V^{(9)}_{ij,n,r}$	$k_9 S^{(9)}_{ij,n+1,r}$	E site tRNA release
$V_{I,r}$	$k_{I,r} R^{(f)} C^{(f)}_{n+6,r}, n = 1$	Translation initiation
$V_{T,r}$	$k_{T,r} S^{T}_{r}$	Translation termination

Assumption 7: Elongation cycle kinetics after ternary complex binding and before Ef-G:GTP binding are first-order with respect to ribosomal states

After nonspecific binding of the ternary complex to the ribosomal A site, the correct codon-anticodon match is verified, which corresponds to flux $V^{(2)}_{ij,n,r}$, and leads to the formation of state 3($S^{(3)}_{ij,n,r}$). State 3 participates in GTP hydrolysis, which corresponds to flux $V^{(3)}_{ij,n,r}$, forming state 4($S^{(4)}_{ij,n,r}$). Ef-Tu:GDP changes position on the ribosome to form state 5 ($S^{(5)}_{ij,n,r}$) and then dissociates from the ribosome to form state 6 ($S^{(6)}_{ij,n,r}$), corresponding to fluxes $V^{(4)}_{ij,n,r}$ and $V^{(5)}_{ij,n,r}$, respectively. Accommodation, corresponding to flux $V^{(6)}_{ij,n,r}$, occurs when the aa-tRNA enters the A site of the ribosome and leads to formation of state 7 ($S^{(7)}_{ij,n,r}$).

Assumption 8: Ef-G:GTP binding kinetics is first-order with respect to free Ef-G:GTP concentration and the ribosomal state that exists before Ef-G:GTP binding

Ef-G:GTP ($G^{(f)}$) binds to state 7 ($S^{(7)}_{ij,n,r}$), corresponding to flux $V^{(7)}_{ij,n,r}$, leading to the formation of state 8 ($S^{(8)}_{ij,n,r}$), which participates in translocation. In addition, we assume that all free Ef-G, before Ef-G:GTP binding to and after Ef-G:GDP release from the ribosome, is in the form of Ef-G:GTP.

Assumption 9: Ribosome translocation also depends on the conditional probability that the codon adjacent to the codon occupied by the front of the ribosome is free, given that the previous codon is occupied by the front of the ribosome

Translocation kinetics are dependent on the conditional probability that the codon adjacent to the codon occupied by the front of the ribosome is free, given that the previous codon is occupied by the front of the ribosome (Eq. 1),

$$U_{n,r} = \begin{cases} \dfrac{C^{(f)}_{n+7,r}}{C^{(f)}_{n+6,r} + \sum_{\sigma} S^{(\sigma)}_{ij,n,r}}, & n \in [1, N_r - (L+1)] \\ 1, & n \in [N_r - L, N_r - 1] \end{cases}. \quad (1)$$

This relationship is adapted from MacDonald et al. (4). Instead of all free codons at position $n+7(C^{(f)}_{n+7,r})$ being available to ribosomes participating in elongation cycles at position n, only the fraction of free codons at position $n+7$ preceded by codons at position $n+6$ occupied by the front of ribosomes are available for ribosome occupancy after translocation. We assume that the flux corresponding to translocation, $V^{(8)}_{ij,n,r}$, is first-order with respect to $U_{n,r}$ and state 8 ($S^{(8)}_{ij,n,r}$).

Assumption 10: The ribosomal state that exists before E-site tRNA release does not have a tRNA present in the A-site

During translocation the codon and tRNA in the P site move to the E site, the codon and tRNA in the A site move to the P site, and the downstream codon in the sequence moves to the A site to form state 9 ($S^{(9)}_{ij,n+1,r}$). The tRNA in the E site dissociates from state 9 to form state 1 of the following elongation cycle, and we assume that this step, corresponding to flux $V^{(9)}_{ij,n,r}$, is first-order with respect to state 9.

Assumption 11: Ribosomes, ternary complexes, Ef-G, and codons are conserved species with constant total concentrations

The total ribosome ($R^{(t)}$), ternary complex ($T^{(t)}_k$), Ef-G:GT(D)P ($G^{(t)}$), and mRNA species (M_r) concentrations are assumed to be constant (time-invariant) and are described by the following conservation equations. Free ribosomes, ternary complexes, Ef-G complexes, and codons are denoted by $R^{(f)}$, $T^{(f)}_k$, $G^{(f)}$, and $C^{(f)}_{n,r}$, respectively, as

$$R^{(t)} = \sum_r \sum_{n=1}^{N_r-1} \sum_{\sigma} (S^{(\sigma)}_{ij,n,r} + S^{T}_{r}) + R^{(f)}, \quad (2)$$

$$T^{(t)}_k = \sum_r \sum_{n=1}^{N_r-1} \left\{ \left(S^{(\sigma)}_{kk,n,r} + 2\sum_{\sigma=2}^{9} S^{(\sigma)}_{kk,n,r} \right) + \sum_{\sigma=2}^{9} S^{(\sigma)}_{ik,n,r} + \sum_{\sigma} S^{(\sigma)}_{kj,n,r} \right\} + T^{(f)}_k, k \in K, \quad (3)$$

$$G^{(t)} = \sum_r \sum_{n=1}^{N_r-1} \sum_{\sigma=8}^{9} S^{(\sigma)}_{ij,n,r} + G^{(f)}. \quad (4)$$

Ribosomes participate in all states at every position on the mRNA (Eq. 2), with the state S^{T}_{r} described in the following assumptions. Ternary complexes k, with $k \in K$ and K the set of ternary complex species, are bound to states where they are cognate to either or both of the A and P site codons (Eq. 3), and Ef-G:GT(D)P is bound to states 7, 8, and 9 of every elongation cycle (Eq. 4). Codons participate in all states in which they occupy either the ribosomal A sites or P sites. Additionally, because ribosomes cover 12 codons on the mRNA, along with the codons occupying the A and P sites the five preceding and following codons are also covered during an elongation cycle (Assumption 2) and are unavailable for participation in other elongation cycles. The total concentration of a codon at a specific position on mRNA r is equal to the concentration of mRNA r (M_r), which is why the free codon concentrations are dependent on M_r. Below are the conservation equations for codons:

$$M_r = \sum_{n}^{n+6} \sum_{\sigma=1}^{8} S^{(\sigma)}_{ij,n,r} + C^{(f)}_{n,r}, n = 1, \quad (5)$$

$$M_r = \sum_{n}^{n+6} \left(S^{(9)}_{ij,n-1,r} + \sum_{\sigma=1}^{8} S^{(\sigma)}_{ij,n,r} \right) + C^{(f)}_{n,r}, n \in [2, N_r - (L+1)]. \quad (6)$$

Assumption 12: Translation initiation is a bimolecular reaction between the ribosome and the initiation site of the mRNA

Translation initiation, corresponding to flux $V_{I,r}$, is considered to be first-order with respect to free ribosomes ($R^{(f)}$) and the free mRNA initiation sites. The initiation site is defined here as the first seven codons of the protein-coding region of the mRNA, with the first codon of the protein coding region as the start codon, and the adjacent noncoding five codons upstream of the start codon. Hence, we assume that the concentration of free mRNA initiation sites is equal to $C^{(f)}_{7,r}$. Translation initiation results in positioning of the ribosomal P site over the start codon.

Assumption 13: Translation termination is a single-step process in which the ribosome dissociates from the mRNA

We introduce the state S^{T}_{r}, which corresponds to the state after the completion of the final elongation cycle and before termination. We assume translation termination kinetics to be first-order with respect to this state, and corresponds to flux $V_{T,r}$.

Mathematical model

The equations that describe the dynamics of the transition between the nine states of the elongation cycle, along with initiation and termination, are as follows:

$$\frac{dS^{(1)}_{ij,n,r}}{dt} = V_{I,r} + V^{(-1)}_{ij,n,r} - V^{(1)}_{ij,n,r}, n = 1, \quad (7)$$

$$\frac{dS^{(1)}_{ij,n,r}}{dt} = V^{(9)}_{ij,n-1,r} + V^{(-1)}_{ij,n,r} - V^{(1)}_{ij,n,r}, n \in [2, N_r - 1], \quad (8)$$

$$\frac{dS^{(2)}_{ij,n,r}}{dt} = V^{(1)}_{ij,n,r} + V^{(-2)}_{ij,n,r} - V^{(2)}_{ij,n,r} - V^{(-1)}_{ij,n,r}, n \in [1, N_r - 1], \quad (9)$$

$$\frac{dS^{(3)}_{ij,n,r}}{dt} = V^{(2)}_{ij,n,r} - V^{(-2)}_{ij,n,r} - V^{(3)}_{ij,n,r}, n \in [1, N_r - 1], \quad (10)$$

$$\frac{dS^{(4)}_{ij,n,r}}{dt} = V^{(3)}_{ij,n,r} - V^{(4)}_{ij,n,r}, n \in [1, N_r - 1], \quad (11)$$

$$\frac{dS^{(5)}_{ij,n,r}}{dt} = V^{(4)}_{ij,n,r} - V^{(5)}_{ij,n,r}, n \in [1, N_r - 1], \quad (12)$$

$$\frac{dS^{(6)}_{ij,n,r}}{dt} = V^{(5)}_{ij,n,r} - V^{(6)}_{ij,n,r}, n \in [1, N_r - 1], \quad (13)$$

$$\frac{dS^{(7)}_{ij,n,r}}{dt} = V^{(6)}_{ij,n,r} + V^{(-7)}_{ij,n,r} - V^{(7)}_{ij,n,r}, n \in [1, N_r - 1], \quad (14)$$

$$\frac{dS^{(8)}_{ij,n,r}}{dt} = V^{(7)}_{ij,n,r} - V^{(-7)}_{ij,n,r} - V^{(8)}_{ij,n,r}, n \in [1, N_r - 1], \quad (15)$$

$$\frac{dS^{(9)}_{ij,n+1,r}}{dt} = V^{(8)}_{ij,n,r} - V^{(9)}_{ij,n+1,r}, n \in [1, N_r - 3], \quad (16)$$

$$\frac{dS^{T}_{r}}{dt} = V^{(9)}_{ij,n+1,r} - V_{T,r}, n = N_r - 2. \quad (17)$$

Equations 7–17 above, together with the conservation equations (Eqs. 2–6), comprise what we call the ZH model. In our computational studies presented in the following sections we also consider the lattice model of protein synthesis first proposed by MacDonald and others (4) and MacDonald and Gibbs (5) and later extended by Heinrich and Rapoport (6), or what we call the MG-HR model. A description of the MG-HR model is included in Appendix A. We performed a sensitivity analysis based on the metabolic control analysis framework (Eqs. 21–26) to determine the sensitivity of steady-state concentrations and fluxes with respect to input parameters for our model. Details of the sensitivity analysis are included in Appendix B.

COMPUTATIONAL STUDIES

We applied our mathematical model of translation elongation to investigate the steady-state properties of translation of the *trpR* gene in *Escherichia coli*. The kinetic data available on the intermediate steps of the *E. coli* elongation cycle and the data available on the intracellular concentrations of the translational machinery make it possible to readily study protein synthesis properties of *E. coli* genes. However, our mechanistic framework is applicable to other organisms. Estimates for the concentration of a single mRNA species r (M_r), the total ribosome concentration available to participate in translation ($R^{(t)}$), the total Ef-G concentration available to participate in translation ($G^{(t)}$), and the total concentrations of ternary complexes available for ribosomal A site binding ($T^{(t)}_k$) used in the computational studies are included in Appendix C.

Protein synthesis properties and polysome size

We investigated how translation rate and control relate to polysome size. We define ribosomal fractional coverage, i.e., ribosome density, as the fraction of mRNAs covered by bound ribosomes, where

$$\rho = \frac{L \sum_n \sum_\sigma S^{(\sigma)}_{ij,n,r}}{M_r N_r}. \quad (18)$$

The ribosomal fractional coverage is proportionate to polysome size. At steady state, for a given ribosomal fractional coverage, a set of pairs of initiation and termination rate constants can be determined. Each of these pairs corresponds to a unique protein synthesis rate. We first determined the pairs of initiation and termination rate constants corresponding to each ribosomal fractional coverage for $0 < \rho < 1$. We hypothesized that at any given growth condition the cell maximizes the protein production rates from each of its mRNAs. Therefore, to determine the relationship between translation rate and polysome size we considered the pair of initiation and termination rate constants corresponding to the maximum specific protein synthesis rate, i.e., the protein synthesis rate per mRNA molecule, for each ribosomal fractional coverage. Fig. 2 *A* shows the specific protein production rate as a function of the fraction of the mRNA covered by ribosomes, ρ. We observe that as ribosomal fractional coverage increases the protein synthesis rate increases, reaches a maximum, and then decreases. Our model predicts that the maximum translation rate of 44 amino acids/s occurs at $\rho = 0.95$. Moreover, the observed range of protein synthesis rates is consistent with experimental reports (27,28).

Rate-limiting steps and polysome size

We applied the control analysis framework to the model to determine if translation is initiation-, elongation-, or termination-limited under different polysome sizes.

We observe that the initiation control coefficients are maximal for low ribosome density. As the ribosome density increases, the elongation control coefficients increase, reach a maximum, and then decrease, and the termination control coefficients are maximum at high polysome sizes (Fig. 2 *B*). We define translation kinetics at a single polysome size to be initiation-limited if $C^v_{k_I} > C^v_{k_E} + C^v_{k_T}$; elongation-limited if $C^v_{k_E} > C^v_{k_I} + C^v_{k_T}$; and termination-limited if $C^v_{k_T} > C^v_{k_I} + C^v_{k_E}$. We observe that translation is initiation-limited for $\rho < 0.5$; elongation-limited for $0.5 < \rho < 0.99$, with elongation control maximal at the same ribosomal fractional coverage that specific protein production rate is maximal; and termination-limited for $\rho > 0.99$.

Rate-limiting steps in the elongation cycle

The flux control coefficients with respect to the rate constants corresponding to the elementary elongation cycle steps were

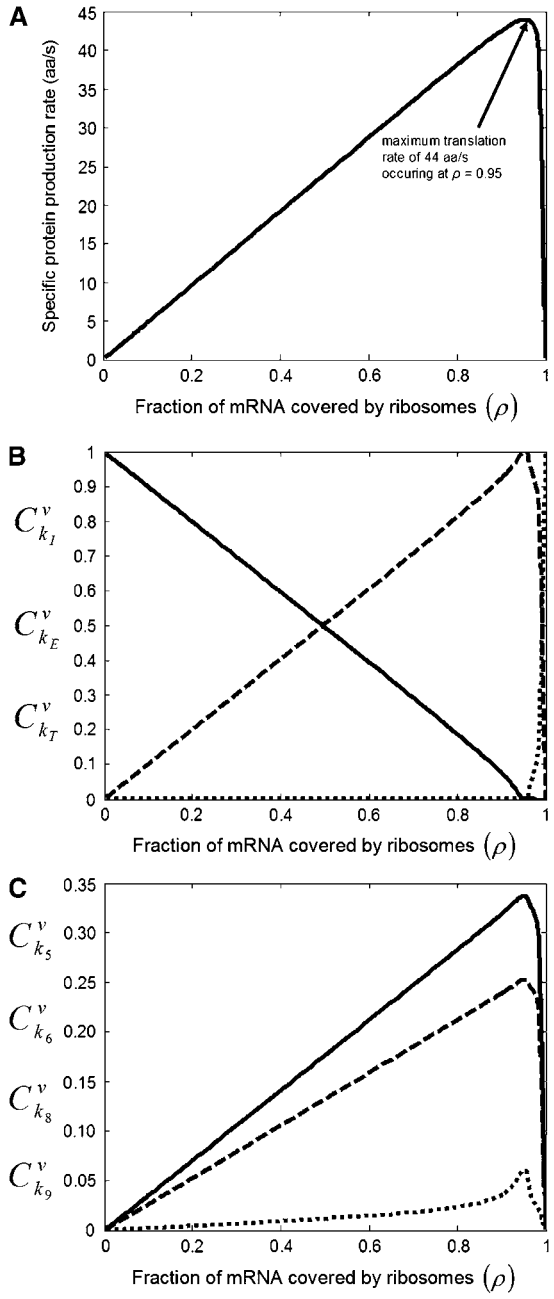

FIGURE 2 Relationships between translation properties and polysome size. (*A*) Specific protein production rate as a function of polysome size. (*B*) Initiation control coefficients, $C^{v}_{k_I}$ (*solid line*), elongation control coefficients, $C^{v}_{k_E}$ (*dashed line*), and termination control coefficients, $C^{v}_{k_T}$ (*dotted line*), as functions of polysome size. (*C*) Elongation cycle intermediate control coefficients with respect to k_5, $C^{v}_{k_5}$ (*solid line*), k_6, $C^{v}_{k_6}$, and k_9, $C^{v}_{k_9}$ (*dashed line*), and k_8, $C^{v}_{k_8}$ (*dotted line*), as functions of polysome size.

also investigated as functions of polysome size. We observe that the control coefficient with respect to the Ef-Tu:GDP release rate constant, $C^{v}_{k_5}$, is maximum (Fig. 2 *C*). This result is consistent with experimental reports, which identify Ef-Tu:GDP release as the rate-limiting step of the elongation cycle (19). Control coefficients for A site tRNA accommodation $(C^{v}_{k_6})$ and E site tRNA release $(C^{v}_{k_9})$ are equal to each other and also high (Fig. 2 *C*). The control coefficient with the third-highest magnitude, $C^{v}_{k_8}$, corresponds to the translocation step (Fig. 2 *C*). The remaining elongation cycle intermediate steps have low control coefficients.

Ribosome distributions

To analyze steady-state ribosomal position and state occupancies, the quantities

$$S_{ij,n,r} = \sum_{\sigma} S^{(\sigma)}_{ij,n,r}/M_r, \tag{19}$$

$$\delta^{(\sigma)}_{n,r} = S^{(\sigma)}_{ij,n,r} / \sum_{\sigma} S^{(\sigma)}_{ij,n,r} \tag{20}$$

are introduced, where $S_{ij,n,r}$ is the total dimensionless concentration of ribosomes with P sites occupying state n regardless of state, and $\delta^{(\sigma)}_{n,r}$ is the fraction of ribosomes at codon n occupying state σ.

Initiation- and elongation-limited kinetics

Under initiation and elongation, limited kinetics ribosomes are uniformly distributed with respect to sequence position throughout the ensemble of mRNAs, and as the polysome size increases, the concentration of ribosomal P sites at each codon increases (Fig. 3 *A*). Most ribosomes at each position occupy the state existing before Ef-Tu:GDP release, state 5 $(S^{(5)}_{ij,n,r})$, and the distribution of states is identical for all ribosomes at each codon (Fig. 3 *B*) for every polysome size. Uniform ribosome distributions are expected under these conditions because once the ribosome binds to the initiation site, movement along the length of the mRNA is relatively unrestricted. Hence, the progress of each elongation cycle is restricted only by the relative magnitudes of the reaction rate constants of the elementary steps. Consequently, most bound ribosomes at each codon occupy state 5 as expected because the control coefficient corresponding to the reaction rate constant for Ef-Tu:GDP release $(C^{v}_{k_5})$ is the highest of all the control coefficients corresponding to the elongation cycle intermediate step rate constants in the initiation- and elongation-limited regimes. In addition, this result demonstrates that our assumption about the total Ef-G concentration free to participate in translation being approximately equal to the total cellular Ef-G concentration is reasonable (this assumption is described in detail in Appendix C). Ef-G is not bound to the ribosome at state 5. Therefore, because most ribosomes participating in translation throughout the initiation- and elongation-limited regimes occupy state 5, and because the initiation- and elongation-limited regimes comprise almost the entire range of polysome sizes, the cellular Ef-G concentration bound to translating ribosomes is negligibly small.

As polysome size increases, ribosomal crowding develops. With ribosomal crowding, it is more likely that the progress of an elongation cycle at position n is limited by the

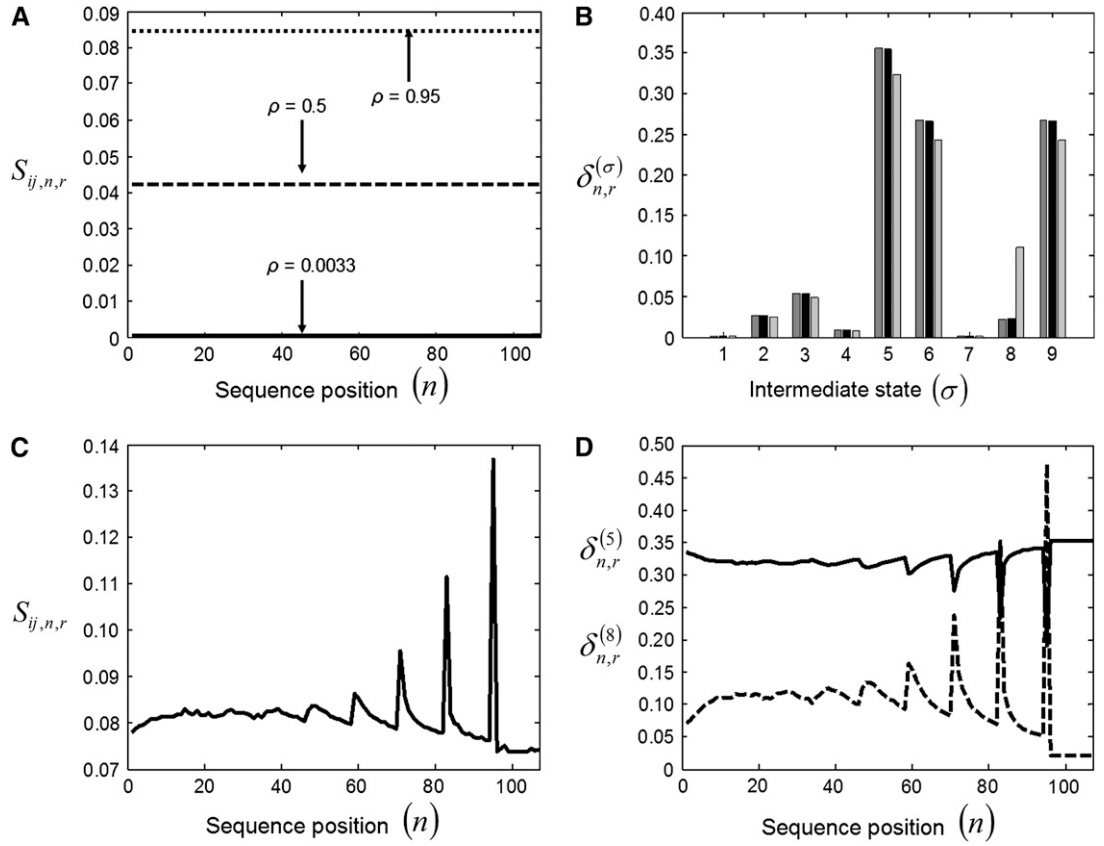

FIGURE 3 Ribosome distributions under initiation- and elongation-limited kinetics. (*A*) Ribosome distributions with respect to codon sequence position for $\rho = 0.0033$ (*solid line*), $\rho = 0.50$ (*dashed line*), and $\rho = 0.95$ (*dotted line*). (*B*) Ribosome distributions with respect to intermediate elongation cycle state for $\rho = 0.0033$ (*dark shading*), $\rho = 0.50$ (*black*), and $\rho = 0.95$ (*light shading*) for all codons along the length of the sequence. (*C*) Ribosome distribution with respect to codon sequence position for $\rho = 0.976$. (*D*) Fraction of ribosomes at each codon position occupying state 5 (*solid line*), and the fraction of ribosomes at each codon position occupying state 8 (*dashed line*) for $\rho = 0.976$.

presence of the tail end of a downstream ribosome occupying the $n+7$ codon position. Presence of the downstream ribosome prevents translocation of the ribosome at position n. Hence, as polysome size increases, more ribosomes at each position occupy state 8 ($S_{ij,n,r}^{(8)}$), the intermediate that exists before translocation (Fig. 3 *B*). We observe that $\rho = 0.95$, the ribosomal fractional coverage corresponding to maximum translation rate, is the maximum ribosomal fractional coverage at which the ribosome distribution with respect to codon position is uniform (Fig. 3 *A*). As the kinetics transition from being elongation-limited to termination-limited in the ribosomal fractional coverage range $0.95 < \rho < 1$, we observe that the ribosome distribution with respect to codon position is not uniform, and that the distribution of states at each codon is not the same for all codons along the length of the sequence (Fig. 3, *C* and *D*). As ribosomal fractional coverage increases from $\rho = 0.95$ ribosome movement becomes restricted at the 3′ end of the mRNA, causing the ribosomes to queue along the length of the chain (Fig. 3 *C*). However, the ribosomal crowding is not high enough in the range of polysome sizes where kinetics transition from being elongation- to termination-limited to cause ribosomes to queue along the entire length of the mRNA, so the ribosome distribution near the 5′ end of the mRNA resembles a uniform distribution (Fig. 3 *C*). Consequently, near the 5′ end of the mRNA the distribution of states at each codon is similar to that in Fig. 3 *B*, with state 5 ribosomal occupancy being the highest (Fig. 3 *D*). However, near the 3′ end of the mRNA ribosomal queuing occurs along the length of the sequence, causing state 8 ribosomal occupancy to increase sharply at positions spaced one ribosome-length apart (Fig. 3 *D*). As a result, the state 5 ribosomal occupancy is similar to the state 5 occupancy under initiation- and elongation-limited conditions, but decreases sharply at these positions (Fig. 3 *D*). The remaining state occupancies (not shown) are also similar to their respective occupancies under initiation- and elongation-limited conditions and decrease sharply at positions where state 8 occupancy is maximal.

Termination-limited kinetics

Under termination-limited kinetics, ribosome movement is strongly restricted at the 3′ end of the mRNA, causing the

ribosomes to queue along the entire length of the chain. Consequently, almost all bound ribosomes have P sites spaced one ribosome-length apart (Fig. 4 *A*). Also, under these conditions ribosomal occupancy of state 8 ($S^{(8)}_{ij,n,r}$) is maximal, with almost all bound ribosomes occupying state 8 at each codon where ribosomal P site occupancy is high (Fig. 4 *B*). The fraction of ribosomes at each codon occupying state 5 is slightly lower under termination-limited conditions than the state 5 occupancy under initiation- and elongation-limited conditions, and approaches zero at each position where ribosomal state 8 occupancy is maximal (Fig. 4 *B*). Ribosomal occupancies of the remaining states (not shown) are also slightly lower under these conditions than their respective occupancies under initiation- and elongation-limited conditions, and also approach zero at each position where ribosomal state 8 occupancy is maximal. The progress of an elongation cycle at position n is more strongly limited by the presence of the tail-end of the proceeding ribosome occupying the $n+7$ codon position under termination-limited conditions than under elongation-limited conditions, resulting in most bound ribosomes occupying state 8.

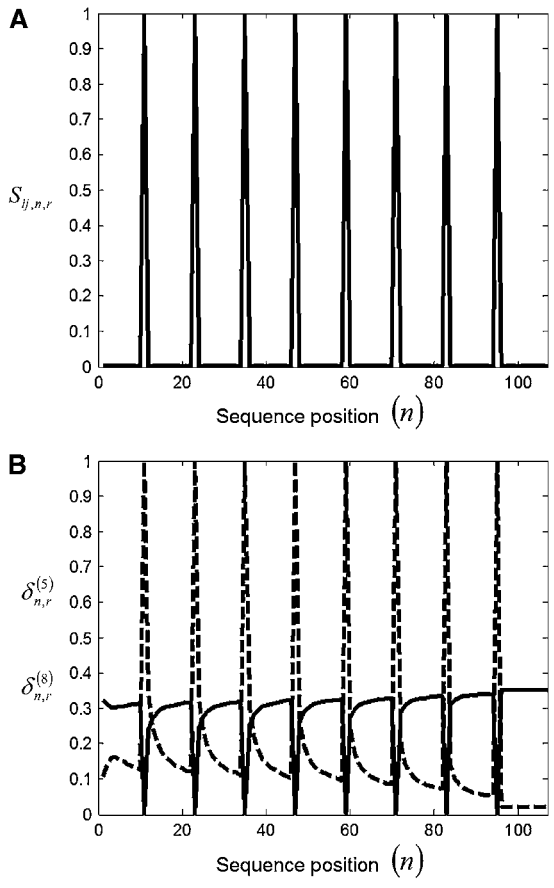

FIGURE 4 Ribosome distributions under termination-limited kinetics for $\rho = 1$. (*A*) Ribosome distribution with respect to codon sequence position. (*B*) Fraction of ribosomes at each codon position occupying state 5 (*solid line*), and the fraction of ribosomes occupying state 8 (*dashed line*).

Effects of ribosome, ternary complex, and Ef-G concentrations on translation rate

We observe that total free ribosome, ternary complex, and Ef-G:GTP concentrations do not limit translation rate of a single gene by examining respective conservation equations (Eqs. 2–4) and control coefficients. Free ribosome ($R^{(f)}$), ternary complex ($T^{(f)}_k$), Ef-G:GTP ($G^{(f)}$), and ribosomal state concentrations ($S^{(\sigma)}_{ij,n,r}$) are made dimensionless by scaling with total ribosome ($R^{(t)}$), ternary complex ($T^{(t)}_k$), Ef-G:GTP ($G^{(t)}$), and mRNA (M_r) concentrations, respectively, allowing the conservation equations for a single mRNA species r to be rewritten as

$$1 = \mu_r \sum_{n=1}^{N_r-1} \sum_{\sigma} (\tilde{S}^{(\sigma)}_{ij,n,r} + \tilde{S}^{T}_{r}) + \tilde{R}^{(f)}, \tag{21}$$

$$1 = \lambda_{k,r} \sum_{n=1}^{N_r-1} \left\{ \left(\tilde{S}^{(\sigma)}_{kk,n,r} + 2 \sum_{\sigma=2}^{9} \tilde{S}^{(\sigma)}_{kk,n,r} \right) + \sum_{\sigma=2}^{9} \tilde{S}^{(\sigma)}_{ik,n,r} + \sum_{\sigma} \tilde{S}^{(\sigma)}_{kj,n,r} \right\} + \tilde{T}^{(f)}_{k}, k \in K, \tag{22}$$

$$1 = \varphi_r \sum_{n=1}^{N_r-1} \sum_{\sigma=8}^{9} \tilde{S}^{(\sigma)}_{ij,n,r} + \tilde{G}^{(f)}, \tag{23}$$

where $\tilde{R}^{(f)}$, $\tilde{T}^{(f)}_k$, $\tilde{G}^{(f)}$, and $\tilde{S}^{(\sigma)}_{ij,n,r}$, are the dimensionless free ribosome, ternary complex, Ef-G:GTP, and ribosome state concentrations, respectively; and μ_r, $\lambda_{k,r}$, and φ_r are dimensionless quantities with

$$\mu_r = M_r / R^{(t)}, \tag{24}$$

$$\lambda_{k,r} = M_r / T^{(t)}_k, \tag{25}$$

$$\varphi_r = M_r / G^{(t)}. \tag{26}$$

Based on the cellular concentrations calculated previously for M_r, $R^{(t)}$, $T^{(t)}_k$, and $G^{(t)}$ we determine that $\mu_r = 2.7 \times 10^{-4}$, $\lambda_{k,r} = [6.9 \times 10^{-5}, 4.3 \times 10^{-3}]$, and $\varphi_r = 5.3 \times 10^{-5}$. Because the concentration of a single mRNA species is low relative to the concentrations of the other available translational components, the ribosome, ternary complex, and Ef-G concentrations sequestered in the ribosomal states on a single mRNA species are low relative to their respective total available concentrations. This finding demonstrates that the coupling that exists between ribosomal states on a single mRNA species due to shared translational resources is low. Hence, when considering the dimensional conservation equations for ribosomes, ternary complexes, and Ef-G:GTP (Eqs. 2–4), $R^{(f)}$, $T^{(f)}_k$, and $G^{(f)}$ are not strong functions of ribosomal state concentrations.

To determine if the total concentrations of the available translational machinery limit the protein synthesis rate, we consider the flux control coefficients with respect to total ribosome, ternary complex, and Ef-G:GTP concentrations. We observe that the flux control coefficients with respect to total ternary complex and Ef-G:GTP concentrations are approximately zero under initiation-, elongation-, and termination-limited kinetics, so the total concentrations of these

translational components do not limit protein synthesis rate. The flux control coefficient with respect to total ribosome concentration is equal to one at low polysome size, and decreases and approaches zero with increasing polysome size. Hence, the total ribosome concentration can significantly impact protein synthesis rate at low polysome size.

A simplified formulation equivalent to the ZH model

To simplify the ZH model and further understand the contributions of each elongation cycle intermediate step to the overall elongation cycle kinetics, we developed a formulation that is an equivalent description of steady-state translation kinetics to the ZH model description of steady-state translation kinetics. By setting the time derivatives equal to zero in Eqs. 7–17 and solving for states 1–8 in terms of state 9, the flux at position n can be written as

$$V_{\mathrm{ij,n,r}} = k^{\mathrm{eff}}_{\mathrm{E,n,r}} S_{\mathrm{ij,n,r}} U_{\mathrm{n,r}} M_{\mathrm{r}}, \tag{27}$$

where

$$k^{\mathrm{eff}}_{\mathrm{E,n,r}} = \frac{1}{U_{\mathrm{n,r}}(\alpha_{1,\mathrm{j}} + \alpha_2 + \alpha_3 + \alpha_4 + \alpha_5 + \alpha_6 + \alpha_7 + \alpha_9) + \alpha_8}, \tag{28}$$

with descriptions of the terms included in Table 3. The magnitudes of the terms in the expression for the effective elongation rate constant (Eq. 28) reflect the influence each elongation cycle intermediate step has over the overall kinetics of the elongation cycle. Similar to the results from the control analysis, the reduced model identifies Ef-Tu:GDP release, accommodation, and E site tRNA release as the elongation cycle intermediate steps that have the greatest influence over elongation cycle kinetics.

The conservation equations for ribosomes and codons are expressed by Eqs. 2, 5, and 6, and conditional probability of ribosome translocation is expressed by Eq. 1, similar to the full model. We have previously identified low flux control coefficients with respect to total ternary complex and Ef-G:GTP concentrations, and therefore we assume in the reduced model that free ternary complex and Ef-G:GTP concentrations are fixed to their respective total available concentrations, leading to $T_{\mathrm{k}}^{(\mathrm{f})} = T_{\mathrm{k}}^{(\mathrm{t})}$ and $G^{(\mathrm{f})} = G^{(\mathrm{t})}$.

With the reduced version of our model the elongation cycle at a given codon is expressed in terms of a single flux (Eq. 27) whose terms map exactly to the MG-HR elongation flux expression (Eq. A4). Both flux expressions at a given codon position depend on the elongation rate constant $k^{\mathrm{eff}}_{\mathrm{E,n,r}}$ (ZH model) and k_{E} (MG-HR model), the probability that the codon is occupied either by the P site (ZH model), $S_{\mathrm{ij,n,r}}$, or front of the ribosome (MG-HR model), $x_{\mathrm{n,r}}$, and the conditional probability governing ribosome movement $U_{\mathrm{n,r}}$ (ZH model) and $W_{\mathrm{n+1,r}}$ (MG-HR model).

Comparison between the ZH and MG-HR models

We used the MG-HR mechanistic framework to determine the specific protein production rate and the initiation, elongation, and termination control coefficients as functions of polysome size (Fig. 5). For the elongation rate constant (k_{E}) we used a value of 5.26 s^{-1}, which we refer to as the characteristic effective elongation rate constant. This value is equal to the effective elongation rate constant discussed previously (Eq. 28) evaluated at $U_{\mathrm{n,r}} = 1$ and at the average free ternary complex concentration of 6.31 μM. The MG-HR model predicts that the maximum translation rate of 29 amino acids/s occurs at $\rho = 0.77$ (Fig. 5 *A*). Also, the MG-HR model predicts initiation-limited kinetics for $\rho < 0.45$, elongation-limited kinetics for $0.45 < \rho < 0.95$, and termination-limited kinetics for $\rho > 0.95$ (Fig. 5 *B*).

Polysome self-organization

We observe two main differences between the ZH model and the MG-HR model in predicting translational behavior with respect to polysome size:

1. The ZH model predicts a higher maximum translation rate than the MG-HR model predicts.
2. The ZH model predicts that the maximum translation rate occurs at a ribosomal fractional coverage that is higher than what the MG-HR model predicts.

In the following sections these differences are addressed by discussing how ribosome occupancies with respect to state and sequence position lead to varying configurations of

TABLE 3 Dimensionless parameters and reduced model terms

Parameter	Expression	Elongation cycle intermediate step	Magnitude
$\alpha_{1,\mathrm{j}}$	$\left[\frac{(k_{-1}+k_2)(k_{-2}+k_3)}{k_2k_3} - \frac{k_{-2}}{k_3}\right]\frac{1}{k_1 T_{\mathrm{j}}^{(\mathrm{f})}}$	Codon-independent binding of the ternary complex	6×10^{-4} – 0.04
α_2	$\frac{k_{-2}+k_3}{k_2k_3}$	Codon-dependent binding	0.005
α_3	$1/k_3$	GTP hydrolysis	0.01
α_4	$1/k_4$	Ef-G:GDP position change on ribosome	0.0015
α_5	$1/k_5$	Ef-G:GDP release	0.067
α_6	$1/k_6$	A site tRNA accommodation	0.05
α_7	$\frac{k_{-7}+k_8}{k_7k_8G^{(\mathrm{f})}}$	Ef-G:GTP binding	3.5×10^{-4}
α_8	$1/k_8$	Translocation	0.004
α_9	$1/k_9$	E site tRNA release	0.05

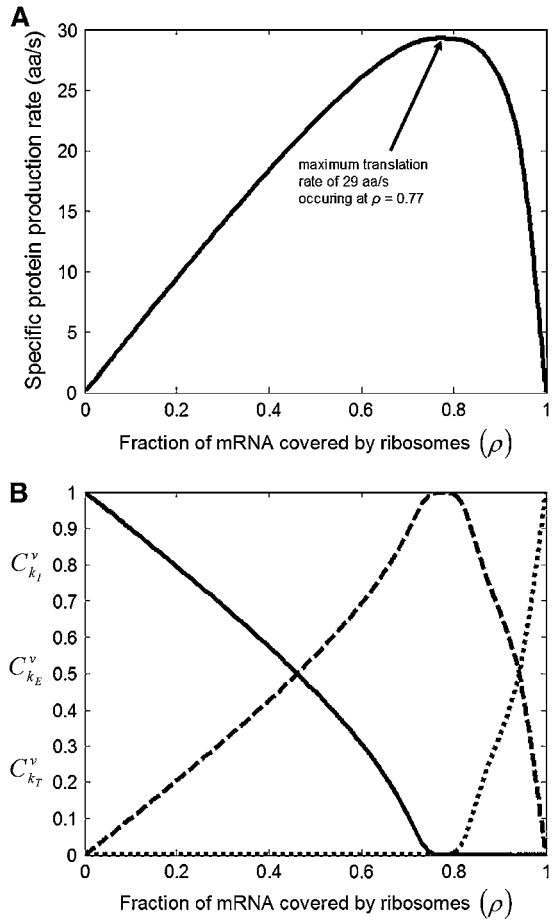

FIGURE 5 Relationships between translation properties and polysome size using the MG-HR model. (*A*) Specific protein production rate as a function of polysome size. (*B*) Initiation (*solid line*), elongation (*dashed line*), and termination (*dotted line*) control coefficients as functions of polysome size.

effective elongation rate constant magnitudes that are specific to different polysome sizes. These results are used to investigate how self-organization of bound ribosomes with respect to the elongation cycle state and position occupancy affects the relationship between translational behavior and polysome size.

Effective elongation rate constants and polysome size

To investigate differences between the results of the ZH model and the MG-HR model we scale the effective elongation rate constants by dividing them by the characteristic effective elongation rate constant, and we compare the scaled effective elongation rate constants derived from our reduced model (Eq. 28) under initiation-, elongation-, and termination-limited kinetics (Fig. 6). We observe that under initiation-limited conditions the effective elongation rate constants along the length of the sequence are approximately equal to

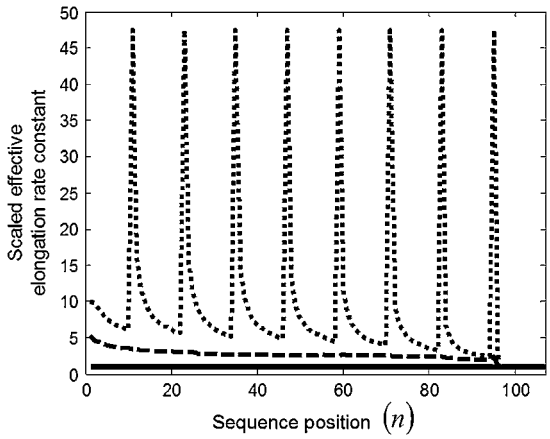

FIGURE 6 Scaled effective elongation rate constants with respect to codon sequence position under initiation-limited ($\rho = 0.0033$, *solid line*), elongation-limited ($\rho = 0.95$, *dashed line*), and termination-limited ($\rho = 1$, *dotted line*) conditions.

the characteristic effective elongation rate constant. Under elongation-limited kinetics the reduced model predicts effective elongation constants approximately equal to five times the characteristic effective elongation rate constant and protein synthesis rates are driven to maximum levels. Under termination-limited conditions the effective elongation constants are approximately equal to 48 times the characteristic effective elongation rate constant at positions spaced one ribosome length apart due to ribosomal queuing along the length of the mRNA, while the rest of the effective elongation rate constants vary between ten and five times as much as the characteristic effective elongation rate constants. In the reduced model the conditional probability ($U_{n,r}$) is in the denominator of the expression for the effective elongation rate constant, $k^{eff}_{E,n,r}$ (Eq. 28), suggesting that $k^{eff}_{E,n,r}$ increases as $U_{n,r}$ decreases due to crowding. At low polysome size, ribosomal crowding on the mRNA is minimal, so $U_{n,r} \approx 1$ and $k^{eff}_{E,n,r}$ is approximately equal to the characteristic effective elongation rate constant. As polysome size increases, ribosomal crowding on the mRNA increases; $U_{n,r}$ decreases causing $k^{eff}_{E,n,r}$ to increase. At high polysome size, ribosomal crowding on the mRNA is maximal and $U_{n,r} \approx 0$, causing $k^{eff}_{E,n,r}$ to approach the magnitude of the translocation rate constant, k_8. Hence, at high polysome size the effective elongation rate constants at positions spaced one ribosome-length apart are approximately equal to k_8. The maximum protein synthesis rate occurs at the polysome size corresponding to the set of effective elongation rate constants that are maximal at each sequence position, while still uniformly distributed along the length of the mRNA.

We observe that the effective elongation rate constants along the length of the mRNA transition as polysome size increases from having magnitudes driving high translation rates to magnitudes that decrease translation rates. To understand how this relationship develops, we investigated effects of relative values of the elongation cycle intermediate

rate constants on the magnitudes of the effective elongation rate constants. Furthermore, we investigated how the altered effective elongation-rate constant magnitudes impact the relationship between translation rate and polysome size (Fig. 7). Because Ef-Tu:GDP release was found to be the elongation cycle intermediate step to contribute the most to the control of the elongation phase over translation rate (Fig. 2 *C*) and to have the highest contribution in the expression for the effective elongation rate constant (Eq. 28, Table 3), the rate constant corresponding to translocation, k_8, was manipulated relative to the rate constant corresponding to Ef-Tu:GDP release, k_5. As k_8 increases relative to k_5, the maximum specific protein production rate increases and the ribosomal fractional coverage at which the maximum specific protein production rate occurs also increases (Fig. 7). Additionally, the relation between translation rate and polysome size does not change when $k_8 > 1000\ k_5$, so the highest possible maximum protein synthesis rate is equal to 48 amino acids/s and corresponds to a ribosomal fractional coverage of 0.98.

Hence, we observe that the magnitudes of the effective elongation rate constants depend both on the level of crowding in the sequence and on how fast the ribosome can be transferred to the next codon in the sequence. As polysome size increases, the number of bound ribosomes to the mRNA increases, and the concentration of the state existing before translocation, state 8, increases (Fig. 3 *B*). This behavior is due to the increased likelihood that the progress of an elongation cycle at position n is limited by the presence of the tail of a downstream ribosome occupying the $n+7$ codon position as previously discussed. The higher the translocation rate constant (k_8), the more ribosomes can be bound to the mRNA without this limitation occurring. As a result, as k_8 increases, the maximum translation rate increases and occurs at increasing polysome sizes because the polysome size can be higher before ribosomal steric effects become significant and limit translation rate. These results demonstrate that it is the configuration of effective elongation rate constant magnitudes with respect to sequence position that lead to optimum translation rate at a specific polysome size. As expected, when we substitute the set of effective elongation rate constants at each polysome size for the elongation rate constants in the MG-HR model, the relationship between protein synthesis rate and ribosomal fractional coverage that is observed is the same as that observed with the ZH model (Fig. 2 *A*).

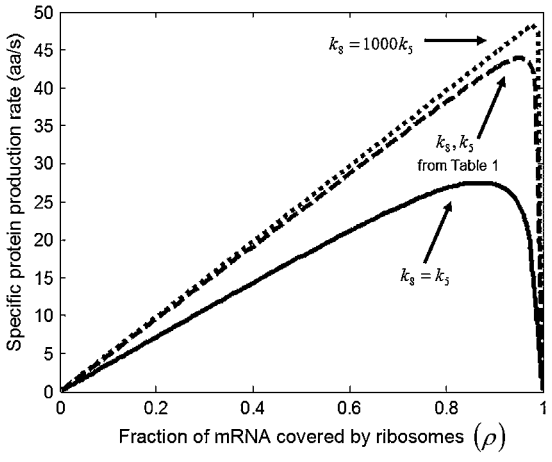

FIGURE 7 Relationships between translation rate and polysome size with k_8 manipulated relative to k_5. Specific protein production rate as a function of polysome size for $k_8 = k_5$ (*solid line*), the k_8 and k_5 values from Table 1 (*dashed line*), and $k_8 = 1000\ k_5$ (*dotted line*).

DISCUSSION

We presented a theoretical analysis of the translation mechanism accounting for the initiation, elongation, and termination phases. Our model of the elongation phase is sequence-specific and includes all the intermediate steps of the elongation cycles taking place at every codon along the length of the mRNA. Consideration of protein synthesis kinetics in the context of polysome size provides insights into quantifying the systemic contributions of the translational components and kinetic parameters to the translational output of genes. As polysome size increases, the ribosomal occupancy with respect to both elongation cycle intermediate and position on the mRNA changes (Figs. 3 and 4). These changes affect the protein synthesis rate (Fig. 2 *A*) and the extent to which the initiation, elongation, and termination kinetic parameters limit translation rate (Fig. 2 *B*).

These results suggest that polysomes self-organize with respect to ribosomal state and sequence position occupancies to achieve maximum translation rates. The relative values of the kinetic parameters corresponding to the intermediate steps of the elongation cycle are such that the polysome size can become very high before ribosomal crowding on the mRNA limits translation rate. We observe that the maximum protein synthesis rate of 44 amino acids/s occurs at a ribosomal fractional coverage of 0.95 (Fig. 2 *A*). Also, by changing the relative magnitudes of the elongation cycle kinetic parameters we observe that the increases in maximum possible translation rate and corresponding ribosomal fractional coverage are not dramatic (Fig. 7), which suggests that the relative reported values for the elongation kinetic parameters are near optimal.

It is important to note that the same set of reaction rate constants were used for the elongation cycle intermediate steps at every codon along the length of the sequence. However, due to the interplay between the level of ribosomal crowding on the mRNA and the contributions of the intermediate elongation cycle steps to the kinetics of the overall elongation cycle, the effective elongation rate constants change with polysome size and sequence position (Fig. 6). The magnitudes of the effective elongation rate constants at a given polysome size determine the translation rate at that polysome size. Additionally, similar translational behavior with respect to polysome size was observed when the relative values of the

elongation cycle kinetic parameters were altered (Fig. 7). Hence, our findings suggest that the behavior we observe is intrinsic to the translation mechanism. In future studies it will be important to incorporate codon-specific kinetic parameters into our model to investigate how translational behavior is affected.

The elongation cycle reaction rate constants used in our model were determined experimentally in vitro, so although we hypothesize that our findings are intrinsic to the translation mechanism, we do not expect that the numerical results we observe are exactly what would be observed in vivo. However, the translation rates predicted by our model compare well with those of in vivo results. According to Neidhardt (27), *E. coli* has a bulk translation rate of 18 amino acids/s. In recent work (29) the bulk initiation rate constant corresponding to this translation rate was determined to be equal to $6 \times 10^4\ M^{-1}\ s^{-1}$. Our model predicts that this initiation rate constant corresponds to a translation rate of 22 amino acids/s, which is a commonly reported value (27). Also, protein synthesis rates as high as 40 amino acids/s have been observed (28), and our model predicts a maximum protein synthesis rate of 44 amino acids/s (Fig. 1 *A*). Hence, this study appears to predict extremely well the translation properties in vivo.

Because the translational behavior for a given ribosomal fractional coverage corresponds to a unique pair of initiation and termination rate constants, we do not necessarily expect a single mRNA species to be able to take on the full ribosomal fractional coverage range. However, a recent study in *Saccharomyces cerevisiae* (3) demonstrates that different mRNA species take on different polysome sizes, and the full ribosomal fractional coverage range is observed. Hence, our mechanistic framework can be used to provide insight into the translation of proteins of high and low expression levels and, subsequently, how cellular resources are allocated for the synthesis of different proteins.

In this study we assume that the total concentrations of ribosomes, ternary complexes, and Ef-G:GTP free to participate in translation are constant. To further investigate allocation of cellular resources and the translational output of genes, our mechanistic framework can be expanded to account for the simultaneous translation of multiple mRNA species. Previous experimental studies on the relative changes in mRNA and protein levels in response to an environmental and/or genetic perturbation (30,31) have shown a nonlinear, not one-to-one, relation between mRNA and protein expression. Also, previous computational studies suggest that this nonlinear relation is due to system-wide competition for ribosomes and tRNAs (7,8). By applying our mechanistic framework to the simultaneous translation of multiple mRNA species, we will be able to understand how the coupling between ribosomal states due to shared translational components relates to system-wide properties.

While some of the conclusions drawn from our studies might be as expected to those experienced with protein synthesis, the proposed computational framework provides a quantitative verification and allows the formulation of hypotheses for the origins of the observed phenomena that mental simulations alone cannot offer. In this investigation we incorporated information about discreet intermediate steps in our framework to make quantitative predictions about the translation mechanism. These mathematical models will allow us to consider each part of the complex biological process and to develop a more complete understanding of translation at the systems level.

CONCLUSIONS

In this work we developed a deterministic, sequence-specific kinetic model of the translational machinery that accounts for all the elementary steps of the translation mechanism. We also performed a sensitivity analysis to determine the effects of the kinetic parameters and concentrations of the translational components on the protein synthesis rate. Moreover, we developed a reduced formulation utilizing effective elongation rate constants that is an equivalent description of steady-state translation kinetics to the ZH model description of steady-state translation kinetics. We determined the following:

1. As polysome size increases translation rate increases, reaches a maximum, and then decreases.
2. Translation kinetics are either initiation- or elongation-limited for almost the entire range of polysome sizes, and are termination-limited at very high polysome sizes.
3. The elongation cycle intermediate step with the most control over a given elongation cycle is Ef-Tu:GDP release, i.e., for the elongation cycle at a given codon, Ef-Tu:GDP release is the most rate-limiting intermediate step.
4. Ribosome distributions with respect to codon position in the initiation- and elongation-limited regimes are uniformly distributed. Ribosome distributions in the termination-limited regime are composed of ribosomal P sites spaced one ribosome-length apart due to queuing that occurs along the length of the mRNA.
5. In the initiation- and elongation-limited regimes ribosomes primarily occupy the state existing before Ef-Tu:GDP release. In the termination-limited regime, ribosomes primarily occupy the state existing before translocation.
6. The maximum protein synthesis rate occurs at the polysome size corresponding to the set of effective elongation rate constants that are maximal at each sequence position, while still uniformly distributed along the length of the mRNA. The configuration of effective elongation rate constants depends on the complex interplay between ribosomal occupancy of elongation cycle intermediate states and ribosome distributions with respect to codon position along the length of the mRNA.

These results were determined without accounting for the competition between mRNA species for translational resources (ribosomes, ternary complexes, elongation factors)

in our mechanistic framework. Future studies will consider the impact of mRNA competition on protein translation properties and conclusions are subject to change.

APPENDIX A: THE MG-HR MODEL OF THE TRANSLATION MECHANISM

In this model, the dynamics of protein synthesis from the mRNA of species r with length N_r codons are described by $(N_r + 1)$ differential equations of the form

$$\frac{d(M_r x_{n,r})}{dt} = V_{I,r} - V_{n,r} \; n = 1, \tag{A1}$$

$$\frac{d(M_r x_{n,r})}{dt} = V_{n-1,r} - V_{n,r} \; n = [2, N_r], \tag{A2}$$

where $M_r x_{n,r}$ is the concentration of codons occupied by the front of the ribosome, $x_{n,r}$ is the probability of each codon n on mRNA r being occupied by the front of the ribosome, and $V_{n-1,r}$ and $V_{n,r}$ are the rates of ribosome movement from codon $n-1$ to n and from n to $n+1$, respectively. The initiation rate is described as

$$V_{I,r} = k_{I,r} R^{(f)} W_{I,r} M_r, \tag{A3}$$

where $W_{I,r}$ is the probability that the initiation site is free $(W_{I,r} = 1 - \sum_{n=1}^{L} x_{n,r})$. The free ribosome concentration $(R^{(f)})$ is a function of the total ribosome and mRNA species concentrations, along with the occupation probabilities of each codon on every mRNA $(R^{(t)} - \sum_r M_r \sum_{n=1}^{N_r+1} x_{n,l})$. The rates of movement of the ribosomes are described by the equations

$$V_{n,r} = \begin{cases} k_E x_{n,r} W_{n+1,r} M_r & 1 \le n \le N_r - L + 1 \\ k_E x_{n,r} M_r & N_r - L + 2 \le n \le N_r \end{cases}, \tag{A4}$$

where k_E is the elongation constant and $W_{n+1,r}$ denotes the conditional probability that codon $n+1$ is free, given that codon n is occupied, formulated as $W_{n+1,r} = \{(1 - \sum_{n=1}^{L} x_{n+1,r})/(1 - \sum_{n=1}^{L-1} x_{n+1,r})\}$. The rate of termination is expressed as

$$V_{T,r} = k_{T,r} x_{N_r+1,r} M_r, \tag{A5}$$

where $k_{T,r}$ is the termination rate constant.

The main difference between our model and the MG-HR model is that our model accounts for all intermediate steps of the elongation cycle, while the MG-HR model treats the elongation cycle as a single step that is dependent on a single elongation rate constant (k_E) that is the same for all codons. In our model we use the position of the ribosomal P site on the mRNA as the reference position of the ribosome, while the MG-HR model uses the position of the front of the ribosome on the mRNA as the reference position of the ribosome.

APPENDIX B: SENSITIVITY ANALYSIS

Sensitivities are quantified using the concentration control coefficients, $C_p^{x_i}$, and flux control coefficients, C_p^{v}, which are defined as fractional concentration and flux changes, respectively, with respect to fractional input parameter changes (21). In this model input parameters include total ribosome, ternary complexes, Ef-G complexes, and mRNA concentrations, along with reaction rate constants. Steady-state mass balances can be expressed with the equation

$$N_R v(x_i, x_d(x_i, p_t), p_r) = 0, \tag{A6}$$

where $\boldsymbol{N_R}$ is the stoichiometric matrix consisting only of rows corresponding to independent species, $\boldsymbol{x_i}$ is the vector of independent species concentrations $(S_{ij,n,r}^{(\sigma)}, S_r^T)$, and $\boldsymbol{x_d}$ is the vector of dependent species concentrations $(R^{(f)}, T_k^{(f)}, G^{(f)}, C_{n,r}^{(f)})$. The vector of fluxes is represented by $\boldsymbol{v}$, the vector of total species concentrations $(R^{(t)}, T_k^{(t)}, G^{(t)}, M_r)$ is represented by $\boldsymbol{p_t}$, and the vector of reaction rate constants $(k_1, k_{-1}, k_2, k_{-2}, k_3, k_4, k_5, k_6, k_7, k_{-7}, k_8, k_9, k_{I,r}, k_{T,r})$ is represented by $\boldsymbol{p_r}$. Using the established (log) linear model formalism (24,32,33), we can linearize the system around the steady state and derive expressions for the control coefficients as

$$C_p^{x_i} = -(N_R V E_i + N_R V E_d Q_i)^{-1} [N_R V E_d Q_t \vdots N_R V \Pi], \tag{A7}$$

$$C_p^{v} = (E_i + E_d Q_i) C_p^{x_i} + [E_d Q_t \vdots \Pi], \tag{A8}$$

where $\boldsymbol{p}$ is the generalized parameter set$(p = [p_t \vdots p_r])$; $\boldsymbol{V}$ is the diagonal matrix whose elements are the steady-state fluxes; $\boldsymbol{E_i}$ and $\boldsymbol{E_d}$ are the matrices of elasticities with respect to independent and dependent species, respectively, defined as the local sensitivities of fluxes to species concentrations; $\boldsymbol{Q_i}$ is the matrix that quantifies the relative abundance of dependent species with respect to the abundance of the independent ones and a second matrix, $\boldsymbol{Q_t}$, is the matrix that quantifies the relative abundance of the dependent species with respect to the levels of their corresponding total moieties; and Π is the matrix of elasticities with respect to reaction rate constants, defined as the local sensitivities of fluxes to these values. Similar to the Summation Theorem (21), we can show that the sum of the control coefficients with respect to the reaction rate constants is equal to one,

$$C_{k_I}^{v} + C_{k_E}^{v} + C_{k_T}^{v} = 1, \tag{A9}$$

where $C_{k_E}^{v}$ in the MG-HR formulation is equal to the fractional change in flux with respect to the fractional change in the elongation reaction rate constant, k_E, of every codon, while $C_{k_E}^{v}$ in our formulation is equal to the sum of the flux control coefficients with respect to the elongation cycle intermediate step reaction rate constants, expressed as

$$\begin{aligned} C_{k_E}^{v} = {} & C_{k_1}^{v} + C_{k_{-1}}^{v} + C_{k_2}^{v} + C_{k_{-2}}^{v} + C_{k_3}^{v} + C_{k_4}^{v} + C_{k_5}^{v} + C_{k_6}^{v} \\ & + C_{k_7}^{v} + C_{k_{-7}}^{v} + C_{k_8}^{v} + C_{k_9}^{v}. \end{aligned} \tag{A10}$$

APPENDIX C: RIBOSOME, TERNARY COMPLEX, EF-G:GTP, AND mRNA ABUNDANCES

The total mRNA concentration in *E. coli* is roughly 6.64 μM (28), and there are 4237 known protein coding regions in the *E. coli* genome (*Escherichia coli* K12, complete genome; National Center for Biotechnology Information, Bethesda, MD). Hence, we estimate the concentration, M_r, of a given mRNA species r by assuming equal mRNA levels for all genes, dividing the total mRNA concentration by the number of genes, and obtaining a concentration of 0.0016 μM. The total concentration of ribosomes in *E. coli* is roughly 30 μM (28) and 80% of the ribosomes are engaged in translation throughout the cell (35). Therefore, the total ribosome concentration engaged in translation is estimated to be 24 μM, and the total ribosome concentration free to participate in translation $(R^{(t)})$ is 6 μM. Ef-G $(G^{(t)})$ is also present in a one-to-one ratio with ribosomes (1), and therefore the total Ef-G concentration is assumed to be 30 μM. Because Ef-G is bound to the ribosome only at states 8 and 9 $(S_{ij,n,r}^{(8)}, S_{ij,n,r}^{(9)})$, we assume that the cellular concentration of ribosomes occupying these states combined is negligibly small. Results of the computational studies confirm that this assumption is reasonable. Therefore, we assume the total Ef-G:GT(D)P concentration free to participate in translation $(G^{(f)})$ to be the total Ef-G concentration $(G^{(t)})$.

The total concentration of tRNA in *E. coli* is roughly 332 μM (28). Relative concentrations of different tRNA species taken from Dong et al. (36), along with the total tRNA concentration, are used to estimate the concentration of each tRNA species. To determine total concentrations of free tRNAs available for ribosomal A site binding $(T_k^{(t)})$, tRNA concentrations participating in elongation cycles throughout the cell must be accounted for and subtracted from total tRNA concentrations. To estimate cellular concentrations of tRNAs sequestered in ribosomal A and P sites, we approximate concentrations of ribosomes

participating in translation with A and P sites occupying different codon species pairs by multiplying the estimated cellular concentration of ribosomes participating in translation (24 μM) by the fractional codon pair frequencies in the protein coding regions of the *E. coli* genome from Boycheva et al. (37). We determine the maximum tRNA concentration to be 23.13 μM, the minimum tRNA concentration to be 0.37 μM, and the average tRNA concentration to be 6.31 μM. The free tRNA concentrations determined are equal to the total ternary complex concentrations because we assume all free tRNAs are in the form of ternary complexes (Assumption 3).

The authors thank Dr. Olke Uhlenbeck, Amit Mehra, and Kevin Keegan for the helpful, in-depth discussions. The authors also thank the two anonymous reviewers for their constructive comments.

This research has been supported by the National Science Foundation through the Quantitative Systems Biotechnology Initiative (CMMI 0425833), and DuPont through a DuPont Young Professor Award to V.H. This research has been supported in part by the National Science Foundation-Integrative Graduate Education and Research Traineeship program ''Dynamics of Complex Systems in Science and Engineering'' (DGE-9987577).

REFERENCES

1. Hershey, J. 1987. Protein synthesis. *In Escherichia coli* and *Salmonella typhimurium*: Cellular and Molecular Biology. F. C. Neidhardt, J. L. Ingraham, K. B. Low, B. Magasanik, M. Schaechter, and H. E. Umbarger, editors. American Society for Microbiology, Washington, DC.
2. Miller, O. L., Jr., B. A. Hamkalo, and C. A. Thomas, Jr. 1970. Visualization of bacterial genes in action. *Science.* 169:392–395.
3. Arava, Y., Y. Wang, J. D. Storey, C. L. Liu, P. O. Brown, and D. Herschlag. 2003. Genome-wide analysis of mRNA translation profiles in *Saccharomyces cerevisiae*. *Proc. Natl. Acad. Sci. USA.* 100:3889–3894.
4. MacDonald, C. T., J. H. Gibbs, and A. C. Pipkin. 1968. Kinetics of biopolymerization on nucleic acid templates. *Biopolymers.* 6:1–5.
5. MacDonald, C. T., and J. H. Gibbs. 1969. Concerning kinetics of polypeptide synthesis on polyribosomes. *Biopolymers.* 7:707–725.
6. Heinrich, R., and T. A. Rapoport. 1980. Mathematical modeling of translation of mRNA in eukaryotes; steady-state, time-dependent processes and application to reticulocytes. *J. Theor. Biol.* 86:279–313.
7. Mehra, A., K. H. Lee, and V. Hatzimanikatis. 2003. Insights into the relation between mRNA and protein expression patterns: I. Theoretical considerations. *Biotechnol. Bioeng.* 84:822–833.
8. Mehra, A., and V. Hatzimanikatis. 2006. An algorithmic framework for genome-wide modeling and analysis of translation networks. *Biophys. J.* 90:1136–1146.
9. Varenne, S., J. Buc, R. Lloubes, and C. Lazdunski. 1984. Translation is a non-uniform process. Effect of tRNA availability on the rate of elongation of nascent polypeptide chains. *J. Mol. Biol.* 180:549–576.
10. Curran, J. F., and M. Yarus. 1989. Rates of aminoacyl-tRNA selection at 29 sense codons in vivo. *J. Mol. Biol.* 209:65–77.
11. Soerensen, M. A., and S. Pedersen. 1991. Absolute in vivo translation rates of individual codons in *Escherichia coli*: the two glutamic acid codons GAA and GAG are translated with a threefold difference in rate. *J. Mol. Biol.* 222:265–280.
12. Kazazian, H. H., Jr., and M. L. Freedman. 1968. The characterization of separated α- and β-chain polyribosomes in rabbit reticulocytes. *J. Biol. Chem.* 243:6446–6450.
13. Rose, J. K. 1977. Nucleotide sequences of ribosome recognition sites in messenger RNAs of vesicular stomatitis virus. *Proc. Natl. Acad. Sci. USA.* 74:3672–3676.
14. Revel, M., and Y. Groner. 1978. Post-transcriptional and translational controls of gene expression in eukaryotes. *Annu. Rev. Biochem.* 47:1079–1126.
15. Dittmar, K. A., M. A. Sorensen, J. Elf, M. Ehrenberg, and T. Pan. 2005. Selective charging of tRNA isoacceptors induced by amino-acid starvation. *EMBO Rep.* 6:151–157.
16. Louie, A., and F. Jurnak. 1985. Kinetic studies of *Escherichia coli* elongation factor Tu-guanosine 5′-triphosphate-aminoacyl-tRNA complexes. *Biochemistry.* 24:6433–6439.
17. Bilgin, N., F. Claesens, H. Pahverk, and M. Ehrenberg. 1992. Kinetic properties of *Escherichia coli* ribosomes with altered forms of S12. *J. Mol. Biol.* 224:1011–1027.
18. Rodnina, M. V., T. Pape, R. Fricke, L. Kuhn, and W. Wintermeyer. 1996. Initial binding of the elongation factor Tu·GTP·aminoacyl-tRNA complex preceding codon recognition on the ribosome. *J. Biol. Chem.* 271:646–652.
19. Pape, T., W. Wintermeyer, and M. V. Rodnina. 1998. Complete kinetic mechanism of elongation factor Tu-dependent binding of aminoacyl-tRNA to the A site of the *E. coli* ribosome. *EMBO J.* 17:7490–7497.
20. Savelsbergh, A., V. I. Katunin, D. Mohr, F. Peske, M. V. Rodnina, and W. Wintermeyer. 2003. An elongation factor G-induced ribosome rearrangement precedes tRNA-mRNA translocation. *Mol. Cell.* 11:1517–1523.
21. Kacser, H., and J. A. Burns. 1973. The control of flux. *Symp. Soc. Exp. Biol.* 27:65–104.
22. Heinrich, R., and T. A. Rapoport. 1974. A linear steady-state treatment of enzymatic chains. General properties, control and effector strength. *Eur. J. Biochem.* 42:89–95.
23. Fell, D. A., and H. M. Sauro. 1985. Metabolic control and its analysis. Additional relationships between elasticities and control coefficients. *Eur. J. Biochem.* 148:555–561.
24. Reder, C. 1988. Metabolic control theory: a structural approach. *J. Theor. Biol.* 135:175–201.
25. Kholodenko, B. N., and H. V. Westerhoff. 1993. Metabolic channeling and control of the flux. *FEBS Lett.* 320:71–74.
26. Hatzimanikatis, V., and J. E. Bailey. 1996. MCA has more to say. *J. Theor. Biol.* 182:233–242.
27. Neidhardt, F. C. 1987. *Escherichia coli* and *Salmonella typhimurium*: Cellular and Molecular Biology. American Society for Microbiology, Washington, DC.
28. Sundararaj, S., A. Guo, B. Habibi-Nazhad, M. Rouani, P. Stothard, M. Ellison, and D. S. Wishart. 2004. The CyberCell Database (CCDB): a comprehensive, self-updating, relational database to coordinate and facilitate in silico modeling of *Escherichia coli*. *Nucleic Acids Res.* 32:D293–D295.
29. Underwood, K. A., J. R. Swartz, and J. D. Puglisi. 2005. Quantitative polysome analysis identifies limitations in bacterial cell-free protein synthesis. *Biotechnol. Bioeng.* 91:425–435.
30. Ideker, T., V. Thorsson, J. A. Ranish, R. Christmas, J. Buhler, J. K. Eng, R. Bumgarner, D. R. Goodlett, R. Aebersold, and L. Hood. 2001. Integrated genomic and proteomic analyses of a systematically perturbed metabolic network. *Science.* 292:929–934.
31. Lee, P. S., L. B. Shaw, L. H. Choe, A. Mehra, V. Hatzimanikatis, and K. H. Lee. 2003. Insights into the relation between mRNA and protein expression patterns: II. Experimental observations in *Escherichia coli*. *Biotechnol. Bioeng.* 84:834–841.
32. Hatzimanikatis, V., C. A. Floudas, and J. E. Bailey. 1996. Analysis and design of metabolic reaction networks via mixed-integer linear optimization. *AIChE J.* 42:1277–1292.
33. Wang, L., I. Birol, and V. Hatzimanikatis. 2004. Metabolic control analysis under uncertainty: framework development and case studies. *Biophys. J.* 87:3750–3763.
34 . Reference deleted in proof.
35. Bremer, H., and P. P. Dennis. 1996. Modulation of chemical composition and other parameters of the cell by growth rate. *In Escherichia coli* and *Salmonella typhimurium.* F. C. Neidhardt, editor. American Society for Microbiology, Washington, DC.
36. Dong, H., L. Nilsson, and C. G. Kurland. 1996. Co-variation of tRNA abundance and codon usage in *Escherichia coli* at different growth rates. *J. Mol. Biol.* 260:649–663.
37. Boycheva, S., G. Chkodrov, and I. Ivanov. 2003. Codon pairs in the genome of *Escherichia coli*. *Bioinformatics.* 19:987–998.